

Ultrafast Wigner transport in quantum wires

Mihail Nedjalkov · Dragica Vasileska ·
Emanouil Atanassov · Vassil Palankovski

Published online: 9 December 2006
© Springer Science + Business Media, LLC 2007

Abstract Two quantum-kinetic models, governing the transport of an initial highly non-equilibrium carrier distribution generated locally in a nanowire, are explored. Dissipation processes due to phonons govern the carrier relaxation, which at early stages of the evolution is characterized by the lack of energy conservation in the collisions. The models are analyzed and approached numerically by a backward Monte Carlo method. The basic difference between them is in the way of treatment of the finite collision duration time. The latter introduces quantum effects of broadening and retardation, ultrafast spatial transfer and modification of the classical trajectories, which are demonstrated in the presented simulation results.

Keywords Wigner transport · Electron-phonon interaction · Ultrafast evolution · Confined system

1 Introduction

The early time dynamics of highly non-equilibrium confined carriers incorporates a number of quantum phenomena,

which are subject of active investigations [1]. Depending on the particular system a variety of interaction mechanisms can influence the carrier relaxation. The electron-phonon scattering processes dominate at low density regimes. The classical Boltzmann transport model adequately describes the electron-phonon kinetics in a wide range of physical conditions. However, the early stages of the evolution are beyond the Boltzmann description: the finite duration time Δ_c of the collisions can not be neglected by the classical assumption for an instantaneous scattering process. A finite Δ_c conflicts with another assumption of the Boltzmann picture: the scattering process is no more local in space. The effect of non-locality becomes important at small spatial scales characterizing the confined systems.

The wave vector space provides a natural representation in spatially homogeneous systems. Model equations of the electron-phonon dynamics are developed in the framework of Green functions [2] or density matrix [3] formalisms. Explicitly or implicitly these models give rise to the Levinson [4] and/or the Barker-Ferry [5] equations. Inhomogeneous systems are described in the whole phase space. In this case, a convenient description is provided by the Wigner formalism which retains along with the phase space also many other classical concepts.

We explore two Wigner function models of the early evolution of carriers interacting with optical phonons in a quantum wire. Quantum-kinetic effect in such systems have been investigated within a density matrix approach [1], or with the help of a Boltzmann-like equation, where the classical δ function is replaced by a Lorentzian [6]. Our approach is based on the generalized electron-phonon Wigner function (GWF) [7]. The reduced (electron) Wigner function f_w is obtained from the diagonal with respect to the phonon coordinates GWF elements. Closed equations for f_w are derived

M. Nedjalkov (✉) · V. Palankovski
Advanced Material and Device Analysis Group,
Institute for Microelectronics, TU Wien,
Gußhausstraße 27–29, A-1040 Wien, Austria
e-mail: nedjalkov@iue.tuwien.ac.at

D. Vasileska
Department of Electrical Engineering, Arizona State University,
Tempe 85287-5706, USA

E. Atanassov
IPP, Bulgarian Academy of Sciences, Acad. G. Bonchev Str.
Bl.25A 1113 Sofia, Bulgaria

by truncation of the coupling with the off-diagonal elements at two different levels of approximation. The derivation will be presented elsewhere.

2 Kinetic models

Three dimensional phonons with wave vector $\mathbf{q}' = (q'_z, \mathbf{q}'_{\perp})$ are considered, an electric field E can be applied along the z direction of the wire. For simplicity it is assumed that carriers remain in a ground state $\Psi(\mathbf{r}_{\perp})$ in the normal plane \mathbf{r}_{\perp} . The obtained models are represented by the equation:

$$\begin{aligned} & \left(\frac{\partial}{\partial t} + \frac{p_z}{m} \nabla_z + eE \nabla_{p_z} \right) f_w(z, p_z, t) \\ &= \sum_{\mathbf{q}'_{\perp}, p'_z} \int_0^t dt' \{ S(p_z, p'_z, \mathbf{q}'_{\perp}, t, t') f_w(\mathcal{Z}(t'), p'_z(t'), t') \\ & \quad - S(p'_z, p_z, \mathbf{q}'_{\perp}, t, t') f_w(\mathcal{Z}(t'), p_z(t'), t') \}, \end{aligned} \tag{1}$$

where

$$\begin{aligned} S(p_z, p'_z, \mathbf{q}'_{\perp}, t, t') &= 2 |F_G(\mathbf{q}')|^2 e^{-\int_{t'}^t \gamma \left(\frac{p_z + p'_z}{2} \right) (\tau) d\tau} \\ & \times \left[n(\mathbf{q}') \cos \left(\int_{t'}^t \frac{(\epsilon(p_z(\tau)) - \epsilon(p'_z(\tau)) - \hbar\omega_{\mathbf{q}'}) d\tau}{\hbar} \right) \right. \\ & \left. + (n(\mathbf{q}') + 1) \cos \left(\int_{t'}^t \frac{(\epsilon(p_z(\tau)) - \epsilon(p'_z(\tau)) + \hbar\omega_{\mathbf{q}'}) d\tau}{\hbar} \right) \right] \end{aligned} \tag{2}$$

F_G denotes the product of the electron-phonon coupling element F with the Fourier transform of $|\Psi|^2$. The models can be considered as inhomogeneous counterparts of the Levinson (L) and Barker-Ferry (B-F) equations, respectively. In the former case $\gamma = 0$, in the latter γ is the common Boltzmann out-scattering rate:

$$\begin{aligned} \gamma(p) &= \sum_{\mathbf{q}''} 2\pi \hbar |F_G(\mathbf{q}'')|^2 \\ & \times \left[(n(\mathbf{q}'') + 1) \delta(\epsilon(p) - \epsilon(p - \hbar q''_z) - \hbar\omega_{\mathbf{q}''}) \right. \\ & \left. + n(\mathbf{q}'') \delta(\epsilon(p) - \epsilon(p + \hbar q''_z) + \hbar\omega_{\mathbf{q}''}) \right]. \end{aligned} \tag{3}$$

We note the modification of the Newton’s trajectory $z(t')$, $p(t')$ by the half of the phonon wave vector $\hbar q'_z = p_z - p'_z$ along the wire:

$$\begin{aligned} \mathcal{Z}(t') &= z - \frac{1}{m} \int_{t'}^t \mathcal{P}_z^-(\tau) d\tau = z(t') + \frac{\hbar q'_z}{2} (t - t') \\ \mathcal{P}_z^-(t') &= p_z - \frac{\hbar q'_z}{2} - eE(t - t') = p_z(t') - \frac{\hbar q'_z}{2} \end{aligned} \tag{4}$$

Equation (4) manifests the nonlocal nature of the electron-phonon interaction: the classical trajectories are generalized by Wigner paths [8]. The basic differences between (1) and the Boltzmann equation are introduced by the time integration on the right hand side and by the cosine function which replaces the energy conserving δ function. The former shows that the evolution is non-Markovian, which gives rise to effects of retardation. The lack of energy conservation causes collisional broadening: the after-scattering energy does not obey the classical selection rule. The interval $\Delta_c = t - t'$ is identified as the collision duration time, introduced by Bordone et al. [9]. Both models consider processes where at t' half of the phonon momentum is transferred to the electron. After Δ_c either the other half is absorbed or the same half is returned. The next collision initiates only after the previous one is completed. The two models differ in the way of treatment of collisions with different duration. While in the L case all collisions are equally treated, in the B-F case these with long correlation times Δ_c are damped by γ in (2).

3 Simulation results

A GaAs quantum wire with 10 nm square cross section has been considered in the numerical experiments. The choice of temperature $T = 0$ K provides a clear reference picture, where classical carriers can only emit phonons and since the constant POP energy form replicas of the initial distribution. The latter is chosen to be Gaussian in both energy and space. A backward Monte Carlo method is used to evaluate directly the Wigner function f_w and its first moments—the density $n(z)$ and the wave vector distribution $f(k_z)$, while t remains implicit:

$$f(k_z) = \int dz f_w(z, \hbar k_z, t); \quad n(z) = \int dp_z f_w(z, p_z, t).$$

To analyze certain numerical aspects f and n are also computed indirectly from the values of f_w .

Figure 1 shows the time evolution of $f(k_z)$ of the two models. The classical evolution forms exact replicas of the initial peak shifted by the phonon energy to the left. The region to the right of the initial peak is forbidden for the classical carriers. The 50fs quantum distribution is very broadened, the appearance of carriers in the classically forbidden region is well demonstrated. At such small times the cosine function in (2) allows scattering to practically all points in the k_z domain. With the increase of the time the kernel in (1) begins to tolerate processes obeying energy conservation. The first replica of the 150fs distributions is already well pronounced but still broadened with respect to the initial condition. The distance between the two peaks, centered at 44 and 50 [10^7 m^{-1}], corresponds to the exact energy conservation. Two spurious

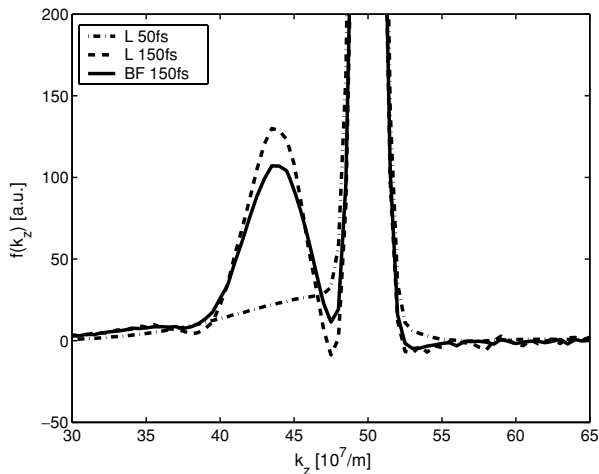


Fig. 1 Wave vector distribution $f(k_z)$, plotted in a window of positive k_z , after 50fs and 150fs evolution time

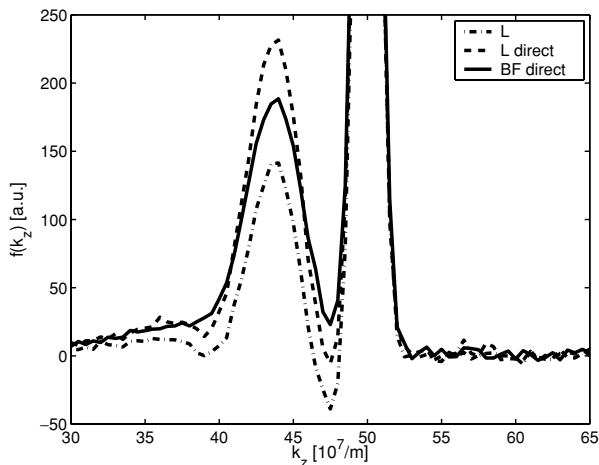


Fig. 2 Broadening and retardation effects after 175fs

effects can be observed: the L distribution becomes negative in the valley, the appearance of carriers in the forbidden region is already missing. The effects are related to the indirect approach: the distributions are obtained from f_w evaluated in 800×260 z and k_z points by a numerical integration on z . The effects exist despite the high precision of computation of f_w and are associated with the fact that with the increase of the time the Wigner function loses the initial smoothness and more points are necessary for a correct quadrature approach.

Figure 2 compares the wave vector distributions after 175fs evolution. The indirect curve becomes fairly unphysical as compared to the directly computed one. Thus a direct evaluation of the physical observables is desirable for larger evolution times. A comparison between the directly computed L and B-F curves demonstrates the main difference between the two models. The finite lifetime γ causes a retardation

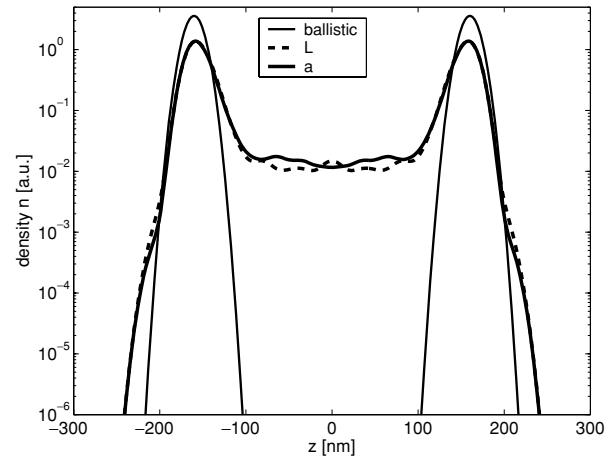


Fig. 3 Electron density after 175fs of evolution time presented in a logarithmic scale

dation of the carrier evolution. The build up of the first B-F replica evolves with a delay with respect to the L counterpart.

The spatial evolution of the carrier density is shown in Fig. 3. The initial distribution centered at the origin splits in two peaks, which move in the positive and the negative directions of the wire. There are no ballistic electrons left around the center. The quantum solutions demonstrate finite density in the central part due to the electrons which lose energy from the collisions. This effect is also a characteristic of the classical model if scattering is enabled. Now we focus on the behavior around the frontiers of the spatial evolution. The front parts of the ballistic curve comprises the fastest classical electrons since the latter can only lose energy by the phonons. The L and B-F solutions show that above and below the ballistic front, at around 230 nm and -230 nm, respectively, there are faster quantum electrons. The latter gained energy from the collisions and reached distances further away from the origin. This effect of ultrafast spatial transfer has been recently reported in [1]. The retardation causes only a small difference in the spatial behavior of the two quantum models.

Finally, we explore the effect of the finite collision duration on the spatial evolution of the carriers. Equation (4) becomes equivalent to the classical trajectory $z(t')$ if the term containing Δ_c is neglected. The density obtained from the B-F model by replacing $\mathcal{Z}(t')$ with $z(t')$ is shown with dashed line in Fig. 4. The general effect is in the modification of the correct carrier density. In particular, it becomes negative exactly where the B-F model shows excess electron density with respect to the ballistic curve. Thus, the neglected term has an important role in maintaining the physical relevance of the quantum model.

A reference to the magnitude of γ shows that few hundred femtoseconds are needed for a good comparison of the two models. Unfortunately the computational demands increase

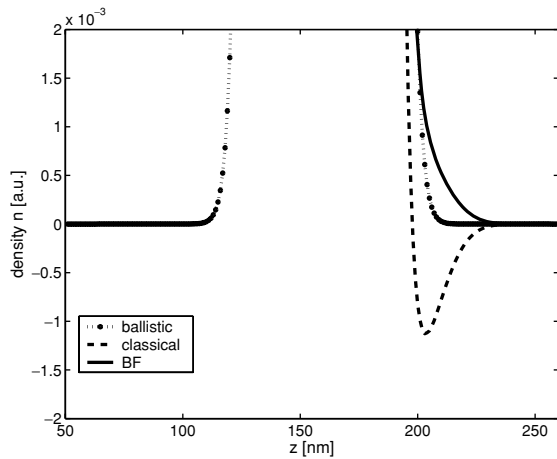


Fig. 4 Electron density after 175fs of evolution time presented in a linear scale

exponentially with the evolution time. The currently under-way application of GRID technologies will probably allow to reach 300fs. Higher times need subtle algorithms or appropriate approximations of the models.

Acknowledgments This work has been partially supported by the Austrian Science Funds, FWF Project START Y247-N13.

References

1. Herbst, M., Glanemann, M., Axt, V., Kuhn, T.: Electron-phonon quantum kinetics for spatially inhomogeneous excitations. *Phys. Rev. B* **67**, 195305 (2003)
2. Rammer, J.: Quantum transport theory of electrons in solids: a single-particle approach. *Rev. Mod. Phys.* **63**, 781 (1991)
3. Schilp, J., Kuhn, T., Mahler, G.: Electron-phonon quantum kinetics in pulse-excited semiconductors: memory and renormalization effects. *Phys. Rev. B* **50**, 5435 (1994)
4. Levinson, I.: Translational invariance in uniform fields and the equation for the density matrix in the wigner representation. *Sov. Phys. JETP* **30**, 362 (1970)
5. Barker, J.R., Ferry, D.K.: Self-scattering path-variable formulation of high field, time-dependent quantum kinetic equations for semiconductor transport in the finite-collision-duration regime. *Phys. Rev. Lett.* **42**, 1779 (1979)
6. Sano, N., Natori, K.: Drift-velocity degradation caused by an electric field during collision in one-dimensional quantum wires. *Phys. Rev. B* **54**, R8325 (1996)
7. Rossi, F., Jacoboni, C., Nedjalkov, M.: A Monte Carlo solution of the Wigner transport equation. *Semicond. Sci. Technol.* **9**, 934 (1994)
8. Pascoli, M., Bordone, P., Brunetti, R., Jacoboni, C.: Wigner paths for electrons interacting with phonons. *Phys. Rev. B* **58**, 3503 (1998)
9. Bordone, P., Vasileska, D., Ferry, D.K.: Collision-duration time for optical-phonon emission in semiconductors. *Phys. Rev. B* **53**, 3846 (1996)